© 2018. Published by The Company of Biologists Ltd | Journal of Cell Science (2018) 131, jcs202416. doi:10.1242/jcs.202416

RESEARCH ARTICLE

SPECIAL ISSUE: PLANT CELL BIOLOGY

# Replication of ribosomal DNA in *Arabidopsis* occurs both inside and outside the nucleolus during S phase progression

**Martina Dvořáčková[1,*], Berta Raposo[2], Petr Matula[3], Joerg Fuchs[4], Veit Schubert[4], Vratislav Peška[1,5], Bénédicte Desvoyes[2], Crisanto Gutierrez[2] and Jiří Fajkus[1,5,6,*]**

## ABSTRACT

Ribosomal RNA genes (rDNA) have been used as valuable experimental systems in numerous studies. Here, we focus on elucidating the spatiotemporal organisation of rDNA replication in *Arabidopsis thaliana*. To determine the subnuclear distribution of rDNA and the progression of its replication during the S phase, we apply 5-ethynyl-2′-deoxyuridine (EdU) labelling, fluorescence-activated cell sorting, fluorescence *in situ* hybridization and structured illumination microscopy. We show that rDNA is replicated inside and outside the nucleolus, where active transcription occurs at the same time. Nascent rDNA shows a maximum of nucleolar associations during early S phase. In addition to EdU patterns typical for early or late S phase, we describe two intermediate EdU profiles characteristic for mid S phase. Moreover, the use of lines containing mutations in the chromatin assembly factor-1 gene *fas1* and wild-type progeny of *fas1*x*fas2* crosses depleted of inactive copies allows for selective observation of the replication pattern of active rDNA. High-resolution data are presented, revealing the culmination of replication in the mid S phase in the nucleolus and its vicinity. Taken together, our results provide a detailed snapshot of replication of active and inactive rDNA during S phase progression.

**KEY WORDS: *A. thaliana* rDNA, Replication, Nucleolus, Flow cytometry, Structured illumination microscopy**

## INTRODUCTION

Ribosomal RNA genes (rDNA) are organised into long repetitive clusters, containing a major fraction of inactive genes intermingled with a minor fraction of actively transcribed genes, forming the nucleolus (Beven et al., 1995; Brown and Gurdon, 1964; Ochs et al., 1985; Pruitt and Meyerowitz, 1986). During DNA replication, the nuclear architecture requires a conformation that enables genome duplication as well as the maintenance of cellular processes, such as the extensive transcription of rDNA needed for ribosome biogenesis during S phase. Most nuclear processes are regulated in a spatiotemporal manner, and replication of rDNA is not an exception (Dimitrova, 2011; Schubeler et al., 2002; Smirnov et al., 2014). A radial model of chromatin organisation was described in mammalian cells, in which gene-rich areas are more centrally localized and each chromosome territory occupies a preferential place in the nucleus consistent with its transcriptional activity (Cremer et al., 2001; Kalhor et al., 2012; Lukášová et al., 2002; Schardin et al., 1985). Gene-rich regions belong to early replicating domains, whereas inactive regions replicate late in S phase (Berger et al., 1997; Lima-de-Faria and Jaworska, 1968; Watanabe et al., 2000). By contrast, the chromosomes of *Arabidopsis thaliana* are mainly randomly distributed within interphase nuclei and the distinct chromocentre-forming gene-poor heterochromatin regions are localized at the nuclear periphery (Pecinka et al., 2004; Schubert et al., 2012).

Ribosomal genes are the most abundant genes in the majority of genomes, and typically only a small fraction of them shows transcriptional activity (Conconi et al., 1989; Dietzel et al., 1999; Grummt and Pikaard, 2003; Miller and Knowland, 1972). The spatial separation of active and inactive ribosomal genes is achieved by the formation of the nucleolus around active genes which contain all necessary components to process nascent rRNA (Dhar et al., 1985; Ochs et al., 1985; Pendle et al., 2005). In the nucleolus, as also shown recently for mammals (Smirnov et al., 2014), further compartmentalisation occurs, which avoids the collision between ongoing replication and transcription. However, since active and inactive copies are adjacent or even intermingled, their complete experimental separation is problematic.

In this study, we focus on the replication of rDNA (45S rDNA) in the model plant *A. thaliana*. Replication of rDNA in other model systems was shown to occur during most parts of the S phase, with the active rDNA fraction replicating in the first half of the S phase at the nucleolar periphery and the inactive genes at later stages (mid S and late S) inside the nucleolus (Balazs and Schildkraut, 1971; Berger et al., 1997; Dimitrova, 2011; Smirnov et al., 2014).

The *A. thaliana* genome is very compact, and rDNA represents one of the most abundant repeats, comprising ∼4% of the genome. Loci of rDNA contain 500–750 copies per haploid genome (Pruitt and Meyerowitz, 1986) and locate on chromosomes 2 and 4, adjacent to the telomeres (Copenhaver and Pikaard, 1996). Their transcriptionally inactive fraction, together with the pericentromeric heterochromatin, participates in the formation of condensed chromocentres, from which active rDNA genes loop out (Fransz et al., 2002). Mutations in the chromatin assembly factor-1 genes (*fas1* or *fas2* mutants) that gradually lose rDNA revealed that only ∼10–20% of rDNA was sufficient for cell viability in *A. thaliana* (Mozgova et al., 2010; Pavlistova et al., 2016). As shown by expression analysis of individual rRNA variants, in *fas1* and *fas2* mutant plants active rDNA copies are being lost first and then replaced by originally inactive copies, which move to the nucleolus,

[1]Laboratory of Molecular Complexes of Chromatin, Mendel Centre for Plant Genomics and Proteomics, CEITEC, Masaryk University, Kamenice 5, Brno 62500, Czech Republic. [2]Department of Genome Dynamics and Function, Centro de Biología Molecular Severo Ochoa, CSIC-UAM, Nicolás Cabrera 1, Madrid 28049, Spain. [3]Department of Computer Graphics and Design, Faculty of Informatics, Masaryk University, Botanická 554/68a, Brno 60200, Czech Republic. [4]Breeding Research Department, Leibniz Institute of Plant Genetics and Crop Plant Research (IPK) Gatersleben, Corrensstrasse 3, Stadt Seeland D-06466, Germany. [5]Department of Cell Biology and Radiology, Institute of Biophysics ASCR, v.v.i., Královopolská 135, Brno 61265, Czech Republic. [6]Laboratory of Functional Genomics and Proteomics, National Centre for Biomolecular Research, Faculty of Science, Masaryk University, Kotlářská 2, Brno 61137, Czech Republic.

*Authors for correspondence (dvorackova.martina@gmail.com; jiri.fajkus@ceitec.muni.cz)

**Received 10 February 2017; Accepted 6 April 2017**

Journal of Cell Science (2018) 131, jcs202416. doi:10.1242/jcs.202416

become activated and undergo large reduction (Mozgova et al., 2010; Pontvianne et al., 2013). Also, the translocation of rDNA to the nucleolar interior is associated with decreased methylation of the rDNA promoter, confirming that nucleolar rDNA is actively transcribed (Pontvianne et al., 2013). Plants carrying *fas1* or *fas2* mutations, or particular subpopulations of wild-type (WT) lines segregated from heterozygous plants after *fas1*×*fas2* crosses (Mozgova et al., 2010; Pavlistova et al., 2016), represent a unique model system to analyse active rDNA without the presence of a high abundance of inactive genes. We took advantage of these plant lines to uncover the spatiotemporal distribution of replicating rDNA, and thus extended the limited number of studies performed on this topic so far (Hernandez et al., 1988; Jasencakova et al., 2001). As mentioned, plant rDNA often associates with the nucleolus, which in actively dividing plant cells occupies the majority of the nuclear volume (Beven et al., 1995; Dvořáčková et al., 2010; Pendle et al., 2005). Remarkably, studies pursuing replication in *A. thaliana* have not considered the nucleolus as a place of DNA replication thus far (Hayashi et al., 2013; Kotogany et al., 2010; Yokoyama et al., 2016). In *A. thaliana*, most authors discriminate only two stages of S phase, early and late, or present the middle S (mid S) as a minor S phase time point (Lee et al., 2010). The S phase in other model plant systems, such as field bean, maize and barley, is subdivided into three stages: early, middle and late S phase (Bass et al., 2014, 2015; Jacob et al., 2014; Jasencakova et al., 2001); and in maize, nucleolar replication was recently described (Bass et al., 2015).

In this study, we present a modified protocol allowing the successful separation of S phase nuclei from *A. thaliana* roots. Relevant protocols have previously been applied by Wear et al. for maize roots and *A. thaliana* cell cultures (Mickelson-Young et al., 2016; Wear et al., 2016), but the procedure has not been optimised for the sorting of S phase nuclei from *A. thaliana* seedlings. Here, we combined fluorescence-activated cell sorting (FACS), rDNA fluorescence *in situ* hybridization (FISH), structured illumination microscopy (SIM) and an implemented set of tools for MATLAB to determine the spatiotemporal distribution of rDNA during replication. We demonstrate that rDNA is replicated inside and outside the nucleolus, and that more rDNA is associated with the nucleolus during the early S phase than during the late S phase. Thus, the nucleolus as the rDNA transcription site is not devoid of replication and, in addition, transcription is not shut down during replication. Four different patterns of 5-ethynyl-2′-deoxyuridine (EdU) labelling are observed: two with typical early and late S phase labelling, and two additional intermediate profiles characteristic for progression through early S and mid S phase. Therefore, we suggest that in *A. thaliana*, as in other eukaryotes, three S phase stages can be distinguished (early, mid and late S), based not only on timing but also on the spatial labelling patterns. Moreover, we demonstrate that the majority of transcriptionally active rDNA genes replicate during mid S phase as determined by using plants depleted of inactive rDNA copies.

## RESULTS

### Replication labelling of *A. thaliana* roots with EdU shows four patterns during S phase, some including signals within the nucleolus

Previous studies using microscopic approaches revealed two types of EdU staining in *A. thaliana* roots, homogeneous labelling of the entire nucleus and EdU foci colocalising with the heterochromatic chromocentres (Hayashi et al., 2013; Kotogany et al., 2010; Yokoyama et al., 2016). To reliably assess the progression of rDNA replication, clarification of S phase subdivision was necessary.

Before analysing rDNA replication, we first re-tested the EdU profiles detectable in *A. thaliana* roots, which were used as starting material in this study. Four-day-old roots were labelled with three EdU pulses (40, 60 or 80 min) to check whether the amount of replicating cells was sufficient for further analysis and to estimate the proportion of nuclei with early and late EdU labelling patterns. Since S phase is estimated to last for ∼2.5 h in *A. thaliana* (Hayashi et al., 2013; Yokoyama et al., 2016), the EdU pulses were relatively short to avoid labelling of entire nuclei, which would compromise the detection of the rDNA replication start points in further experiments.

Areas of EdU labelling for all three pulse times were found in the meristematic zone of the root tip, excluding the differentiated part of the columella and lateral root cap (Fig. 1A) and finishing with the elongation zone where endoreduplication starts (Hayashi et al., 2013; Kotogany et al., 2010; Otero et al., 2016). The actual proportion of cells with early and late EdU patterns (counted according to the criteria described above) did not differ with EdU pulse duration and was ∼50% in all cases (Table S1). Observation of the homogeneously EdU-stained nuclei revealed that the EdU pattern is not identical in all of the nuclei, and that four distinct patterns can be differentiated (Fig. 1A,C).

We then analysed the distribution of EdU signal in the two cellular compartments in which ribosomal genes can be found, the nucleus and nucleolus. The nucleolus, which does not stain well with DAPI, is where active rDNA is located (Pontvianne et al., 2013). The data show that EdU is not excluded from the nucleolus (Fig. 1B). Based on these new observations, the replicating nuclei could be categorised into four types according to the patterns of EdU labelling (Fig. 1C, types 1–4): (1) labelling of the entire chromatin except the strongly DAPI-stained chromocentres (cyan arrows) and the nucleoli; (2) homogeneous labelling of the chromatin, including (some of) the chromocentres; (3) labelling of the entire chromatin with markedly increased EdU accumulation at the chromocentres; and (4) labelling of the chromocentres only. The most intense EdU labelling inside the nucleoli was detected in nuclei of types 2 and 3.

### Optimizing the methods for isolation of *A. thaliana* S phase nuclei

The assessment of EdU labelling allowed us to classify the replicating nuclei into four different types. In order to assign each category to a part of the S phase and to explore in which phases the ribosomal genes replicate, we performed FACS of EdU-labelled *A. thaliana* root tip nuclei in combination with rDNA FISH.

Several recent articles have already provided data on the sorting of replicating nuclei of *A. thaliana* and rice tissue cultures (Costas et al., 2011; Kotogany et al., 2010; Lee et al., 2010) or maize and rice excised root tips (Bass et al., 2014, 2015; Wear et al., 2016).

However, sorting replicating nuclei from *A. thaliana* root tips was not as straightforward as expected and required a few important optimisation steps. First, a suitable growth system to obtain large amounts of starting material was needed. We chose a hydroponic system in which a sufficient amount of material can be obtained and processed at the same time. EdU was simply added directly to this system without additional manipulation of the seedlings. By using ∼0.5 g of seeds per experiment, ∼5000–7000 sorted nuclei could be obtained. Such amounts of material are difficult to obtain from mutant lines with decreased seed production, for instance from *fas1* mutants.

Next, EdU detection was optimised. Since a suspension of nuclei is typically used in a flow sorter, nuclei had to be fixed and further

Journal of Cell Science (2018) 131, jcs202416. doi:10.1242/jcs.202416

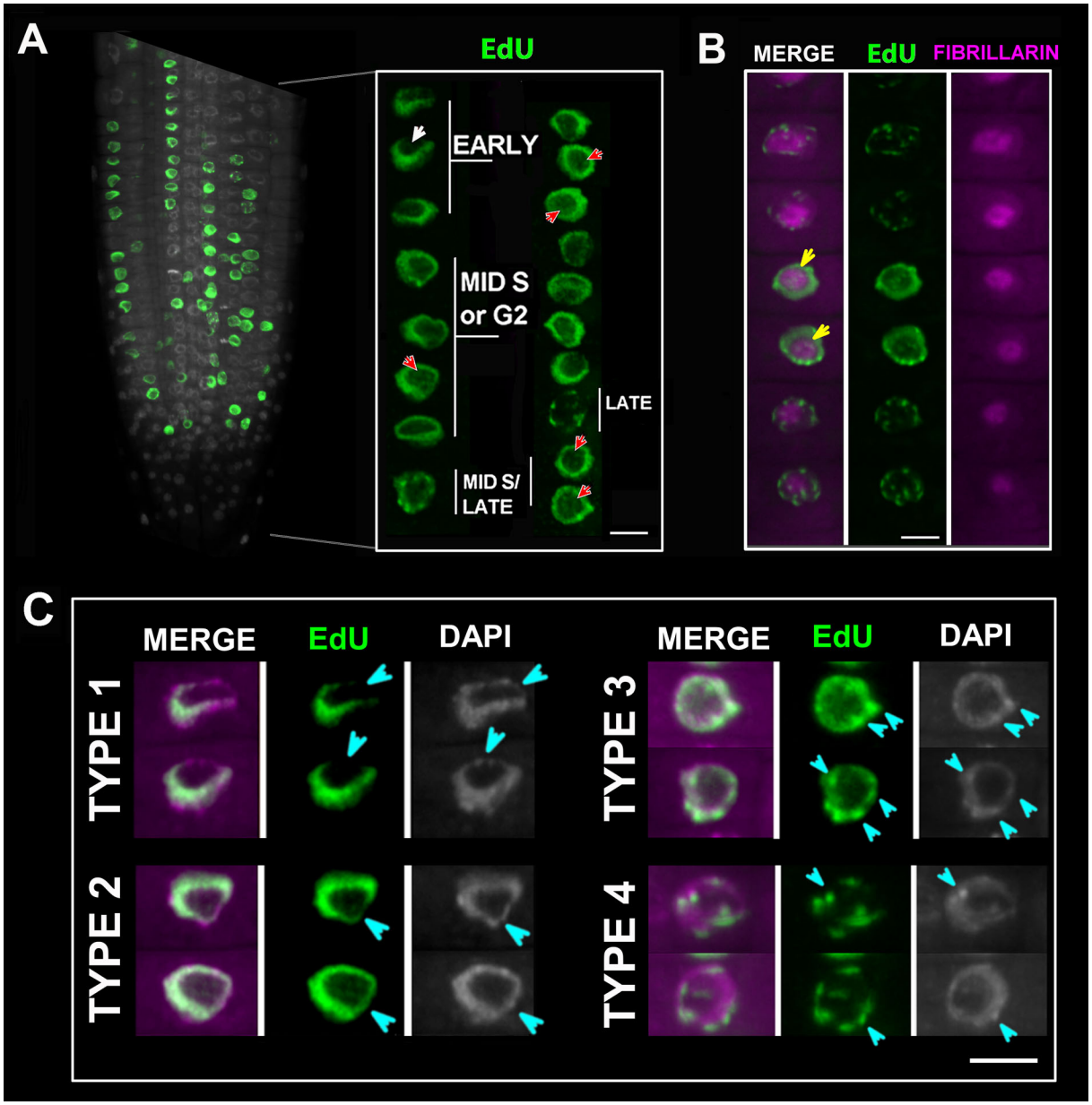


**Fig. 1. Analysis of replication in an *A. thaliana* root incubated for 80 min with EdU.** (A) EdU (AF488, green) labelling in roots, stained with DAPI (grey). The inset image shows two lines of cells in more detail. Red arrows indicate the nucleolar EdU signal; white arrow shows the nucleolus with lower EdU intensity. (B) Simultaneous visualisation of the nucleolus and replication. Cells with nucleolar EdU signals are indicated (yellow arrows). EdU (AF488), green; fibrillarin-YFP, magenta. (C) Individual EdU labelling types (AF488, green); cyan arrowheads point to areas containing chromocentres. Scale bar: 5 µm.

processed in suspension. For EdU detection, the use of a Click-iT kit adapted for flow cytometry was required. The use of picolyl azide instead of azide was necessary as we found that free copper ions interfere with DAPI staining and uncouple the DAPI fluorescence intensity from the ploidy level (Fig. S1A–D). Multiple centrifugation steps required for removing excess fixative and Click-iT components caused unfavourable aggregation of nuclei.

The FACS parameters were adjusted (see Materials and Methods) to achieve optimal resolution to distinguish the typical EdU arch of replicating cells (Fig. 2A). The aggregation of nuclei created a relatively high level of background and decreased the overall efficiency of sorting. However, reasonable amounts of high-quality EdU-labelled nuclei sufficient for microscopy applications were obtained. Gates used to collect fractions of early, mid and late S nuclei are shown in Fig. 2A. The amount of sorted nuclei in late S (1.4% of total nuclei) was higher than the amount obtained in the early S fraction (0.4% of total nuclei) (Fig. 2A), while the mid S fraction corresponded to ∼1.2% of total nuclei. The control sample without EdU showed very little background signal in the Alexa Fluor 488 (AF488) detector (Fig. 2B). An example of sorted nuclei obtained in individual S phase fractions is shown in Fig. 3 and Fig. S2A.

### Classifying *A. thaliana* S phase into individual stages

The EdU signal of sorted nuclei labelled for 40 min was first assessed by confocal microscopy to determine whether the obtained fractions (early, mid and late S phase) show specific EdU patterns. In the early S fraction, nuclei of type 1 and type 2 with relatively low nucleolar signal were usually obtained (Fig. 3A). Type 1 nuclei showing nucleoli and chromocentres mostly devoid of EdU signal

Journal of Cell Science (2018) 131, jcs202416. doi:10.1242/jcs.202416

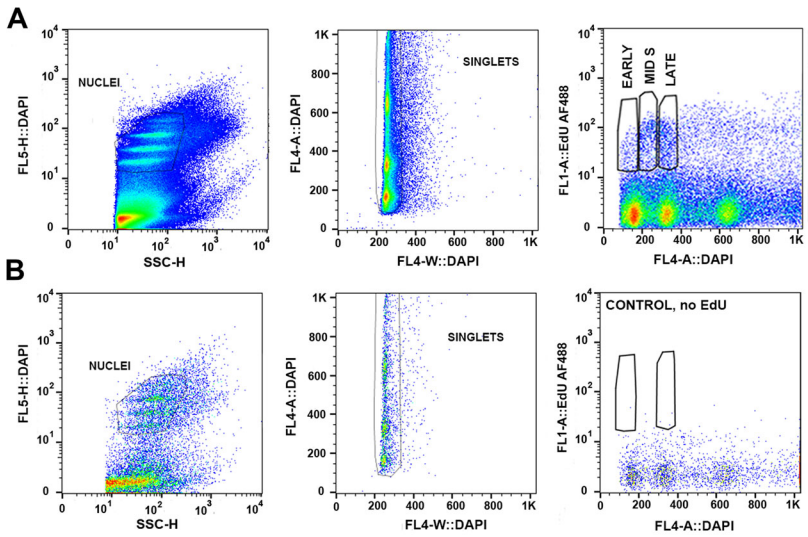


**Fig. 2. Gating strategy used to sort EdU-labelled replicating nuclei of early and late S phase by FACS.** *x*- and *y*-axes represent signal intensity obtained in individual detectors. Detectors used: FL5 (DAPI fluorescence) and SSC to assess quality and gate-stained nuclei, FL4 for singlet nuclei discrimination, and FL1 for EdU fluorescence. A, H, and W represent signal area, height and width, respectively. Left panels show the 2C, 4C and 8C subpopulations of nuclei; middle panels show plots of DAPI width versus area signals for the detection of singlets; right panels show EdU versus DAPI signals (sorting gates used for 2C, 4C and 8C nuclei are indicated). (A) DAPI-stained nuclei after EdU labelling. (B) DAPI-stained nuclei without EdU labelling.

probably corresponded to cells that entered S phase later during the course of the EdU pulse (the DNA had not been labelled for the whole period of the EdU pulse). These cells are likely to represent the very early S phase, while the remaining type 1 nuclei represent advanced early S phase. In comparison, the EdU patterns of the mid S sample showed a certain level of overlap with early S as well as late S fractions (Fig. S2A), as expected for an intermediate phase. It contained a mixture of all four EdU types (Fig. 3A). Compared to the early S fraction, homogeneously labelled mid S nuclei showed an increased nucleolar EdU signal. This difference became more profound when EdU was applied for 80 min (Fig. S2B). Thus, the type 2 nuclei likely represent the boundary between early S and mid S, and the intensity of nucleolar staining in these nuclei reflects the progression into mid S phase.

Finally, in the late S fraction ∼50% of the nuclei were of type 4, and the remaining nuclei showed complete EdU labelling (whole nucleus and speckles) corresponding mostly to type 3 and, to a lesser extent, to type 2 (Fig. 3A).

In conclusion, *A. thaliana* root nuclei can be sorted by EdU labelling. When sorting is combined with microscopic analysis, very efficient separation of two fractions, early S and late S, can be achieved. The mid S fraction typically contains a mixture of nuclei of all of the different EdU patterns.

## rDNA replicates in four steps

To determine when ribosomal genes start to replicate, we sorted nuclei after a 40 min EdU pulse, hybridised them with fluorescently labelled rDNA, and analysed samples by conventional confocal microscopy. Nuclei were then classified into the four different EdU pattern types described above (Fig. 1C). The advantage of performing a short EdU pulse is that it limits the time window in which the replicating DNA incorporates EdU and increases the resolution for the detection of the replication start point.

As shown in Fig. 3B,C, ribosomal genes did not colocalise with EdU labelling at the very beginning of the S phase (type 1 nuclei, very early). In type 1 and 2 nuclei, increasing colocalisation between the EdU signal and rDNA was detected, outside the nucleoli as well as at nucleolar rDNA sites (Fig. 3B,C). These data indicate that initiation of rDNA replication does not occur at the very beginning of the S phase but soon after. In some type 2 nuclei, nearly all rDNA loci appeared to be simultaneously EdU labelled (Fig. 3B). Type 3 cells also showed remarkable EdU labelling of rDNA, similar to type 2 nuclei, but EdU became more concentrated at chromocentres (Fig. 3B,C). Finally, in type 4 nuclei, rDNA replication was restricted to condensed foci, in parallel to the replication of heterochromatic chromocentres, as expected for late S phase. At this point, the nucleolar rDNA fraction was no longer EdU labelled.

As expected for an intermediate labelling pattern, the difference in EdU labelling between type 2 and 3 nuclei was less profound than the difference between type 1 and 4 nuclei. In addition, type 2 and 3 nuclei showed a relatively high level of replicating rDNA within and outside the nucleolus. The remarkable nucleolar labelling suggests that the nucleolus, as the site of rDNA transcription, is not devoid of replication. When ongoing rDNA transcription was tested by EdU labelling, all root tip cells were labelled (Fig. S3).

Taken together, these analyses suggest that rDNA replicates during the whole S phase, except for at its very beginning.

## Detailed analysis of rDNA replication

The analysis of rDNA replication using confocal microscopy provided only an overall idea about the timing of rDNA replication. To determine the distribution of rDNA within and outside the nucleolus during the S phase, the distribution of replicating rDNA, and the replication timing of active rDNA genes present in the nucleolus, we used spatial SIM. A doubling of resolution (super-resolution) can be achieved with SIM, and we combined this technique with detailed image analysis to improve data evaluation. When re-analysing the 40 min EdU-labelled nuclei (Fig. S2C), a relatively low degree of EdU/rDNA colocalisation was detected in the nucleolus (only three of 21 cells showed more than 50% replication in the nucleolus), regardless of a relatively high proportion of nucleolar rDNA signal. Based on these observations, we next performed EdU labelling for 80 min to improve the visualisation of the nucleolar EdU signal required for a reliable colocalisation assessment.

### The abundance of the nucleolar rDNA fraction varies during the S phase

The transcriptionally active rDNA fraction, representing ∼10–20% of the total rDNA (Mozgova et al., 2010), is located within the nucleolus (Pavlistova et al., 2016; Pontvianne et al., 2013). To determine whether this proportion is maintained during S phase, the intensity of the rDNA hybridisation signal was measured in the nucleolus and compared to the signal obtained in other parts

Journal of Cell Science (2018) 131, jcs202416. doi:10.1242/jcs.202416

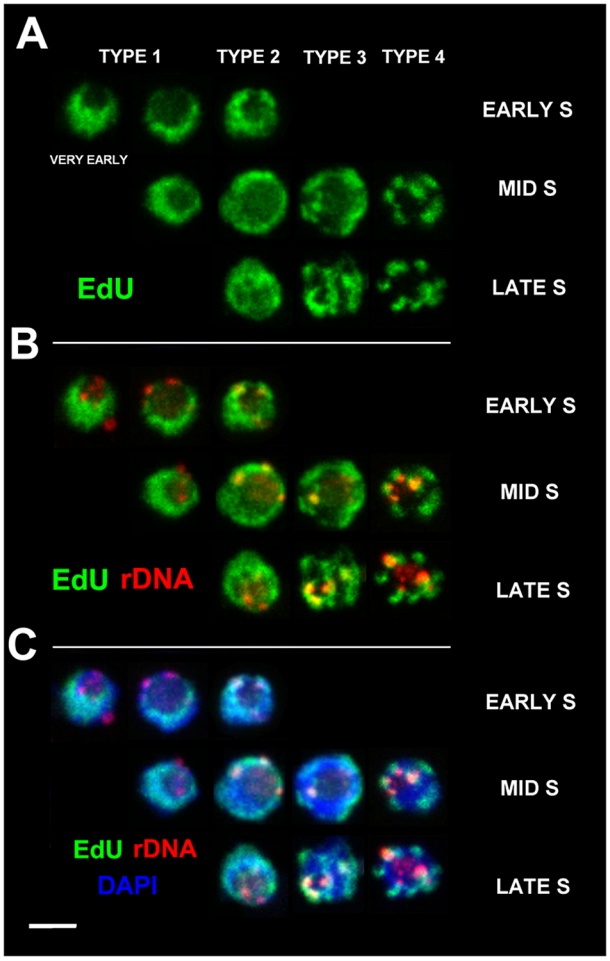


**Fig. 3. rDNA replicates mainly during mid S phase.** Root cells were EdU labelled, and isolated nuclei were sorted according to their EdU incorporation and DAPI staining into three fractions: early, mid and late S. Nuclei were hybridised with a 45S rDNA probe. Maximum intensity projections of nuclei from selected confocal *z*-stacks are shown. Scale bar: 5 µm. (A) EdU-labelled nuclei (AF488, green). (B) Overlay of EdU (AF488, green) and rDNA (AF594, red). (C) Overlay of EdU (AF488, green), rDNA (AF594, red) and DAPI (blue). Type 1: rDNA does not replicate (very early) or only a low level of rDNA replication is detected. Type 2: rDNA starts to replicate in the nucleolus as well as in condensed rDNA loci. Increased nucleolar staining and replication in the chromocentres indicate progression into mid S phase. Type 3: rDNA replication in the nucleus and nucleolus, more EdU is accumulated in foci. Type 4: rDNA replication in condensed chromocentres, the nucleolus is excluded from labelling. This type represents the typical late replication pattern.

of the nucleus. The regions of the nucleus and nucleolus were semiautomatically segmented based on the absence of DAPI staining (see Materials and Methods). In this segmentation tool, signals inside the nucleolar cavity were considered nucleolar, while those occurring at the nucleolar surface (nucleolus associated) were considered extranucleolar. We found that >40% of the rDNA is localized inside the nucleolus during early S (Fig. 4) in the majority of early S phase nuclei (14/22) (Table 1). As the cells progress into mid and late S the sample becomes more heterogeneous, reflecting a more dispersed arrangement of the rDNA (Table 1). During mid and late S, the proportion of nucleolar rDNA decreases to ∼20% (Fig. 4 and Table 1). Thus, it seems that the spatial organisation of rDNA changes dynamically during replication.

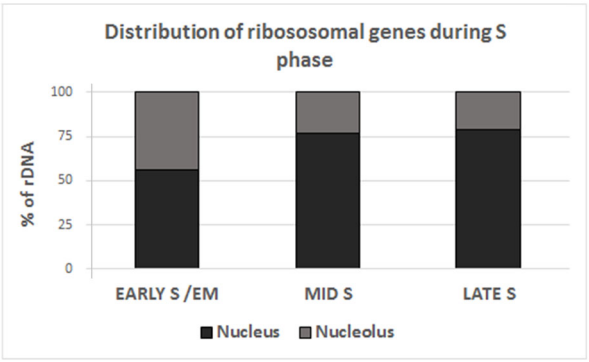


**Fig. 4. Changes in the distribution of rDNA during the S phase.** Percentage of rDNA inside (grey) or outside (black) the nucleolus during the S phase, as assessed by FISH of flow-sorted nuclei. Early S/EM, early S phase and early to mid S phase. The number of analysed cells is provided in Table 1.

### Replication of transcriptionally active rDNA genes occurs in intra- and extranucleolar regions

The aim of the following experiments was to determine the distribution of replicating rDNA and the replication timing of active rDNA genes present in the nucleolus. For this purpose we used *fas1* mutant plants, as well as specific WT lines, containing reduced rDNA amounts. The majority of ribosomal genes in these lines are actively transcribed, as described in detail previously (Mozgova et al., 2010; Pavlistova et al., 2016; Pontvianne et al., 2013). Based on rDNA FISH, most of the rDNA in the nuclei of the low rDNA copy lines appears to be intranucleolar (Pavlistova et al., 2016; Pontvianne et al., 2013). When we analysed rDNA FISH signals by SIM and quantified, most of the nuclei revealed 40–70% of the rDNA inside the nucleolus (Table S2). Because rDNA signals were not observed in the nucleoplasm, the remaining signals were on the nucleolar surface and thus nucleolus associated (but recognised as extranucleolar by the segmentation tool).

When we evaluated rDNA replication by assessing colocalised pixels of the EdU and rDNA FISH signals, we observed that the replication of active rDNA appeared to start in early S phase and progressed during mid S phase, when the first EdU labelling was detected in the chromocentres (Fig. 5A,B). The initiation of rDNA replication at chromocentres represents a marker of mid S phase (Fig. 5A,B). During mid S phase, the total level of replicating rDNA fluctuated between 40% and 90%, and replication usually also occurred inside the nucleolus (Table S3). Although colocalisation analysis showed that some mid S phase nuclei replicated almost the entire nucleolar fraction (≤95%), some small areas were still free of EdU labelling, indicating that not all rDNA copies replicate at the same time (Fig. 5C).

In addition, SIM revealed that active rDNA inside the nucleolus was not completely decondensed, but formed a network-like structure interrupted by more condensed foci, usually brightly

**Table 1. Changes in the distribution of rDNA during the S phase**

| | Nuclei in each category (%) | | |
|---|---|---|---|
| % of nucleolar DNA | Early S/EM | Mid S | Late S |
| <20 | 0 | 47 | 42 |
| 20–30 | 0 | 29 | 35 |
| 30–40 | 36 | 24 | 19 |
| >40 | 64 | 0 | 4 |
| Total number of nuclei | 22 | 17 | 26 |

Early S/EM, early S and early to mid S.

Journal of Cell Science (2018) 131, jcs202416. doi:10.1242/jcs.202416

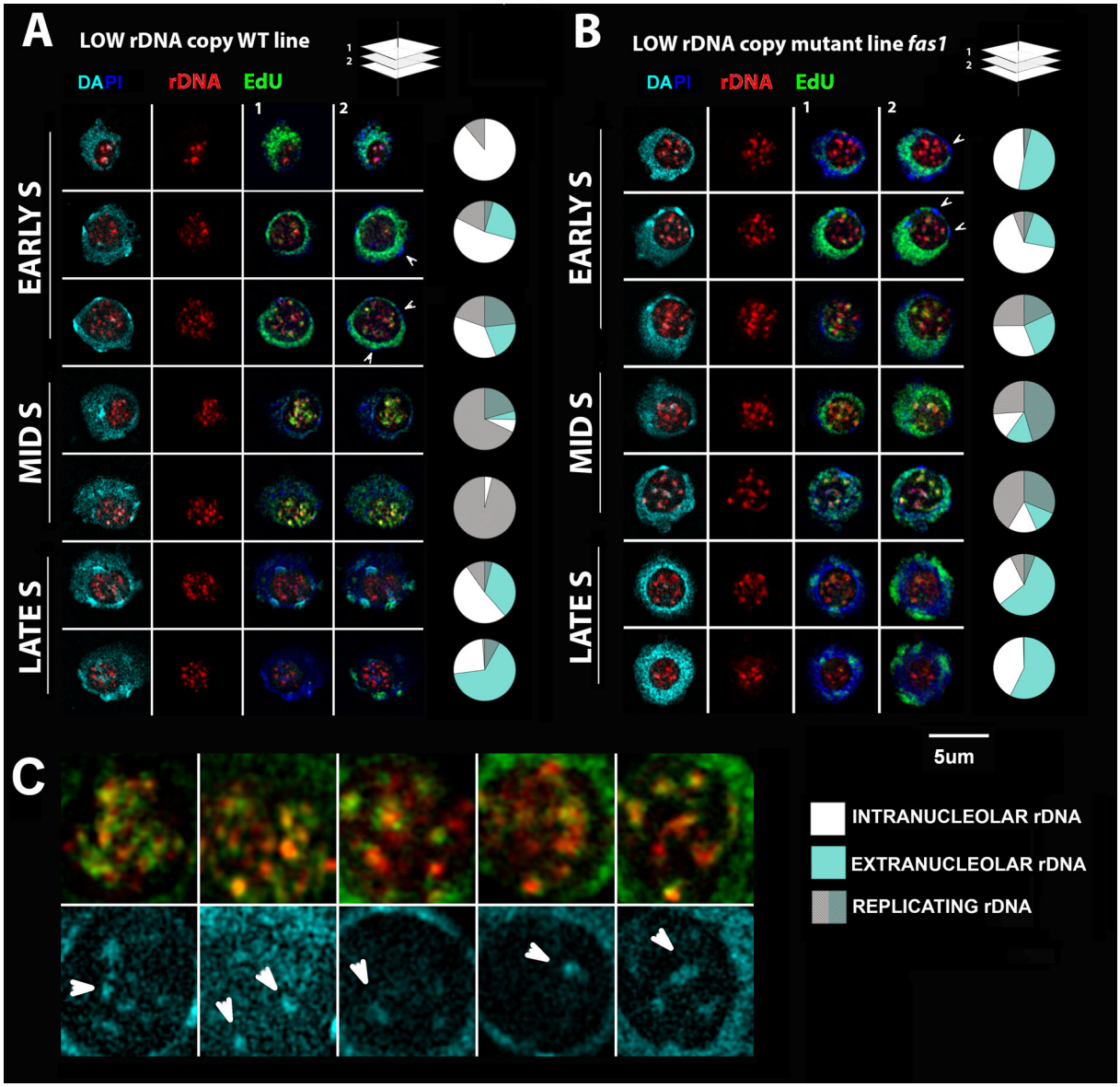


**Fig. 5. Active rDNA replicates inside and outside the nucleolus during the early and mid S phase in low rDNA copy number WT and *fas1* lines.** DAPI (cyan/blue), rDNA (AF594, red) and EdU (AF488, green) images of nucleoli. (A,B) In the DAPI and rDNA overlay (first column) and rDNA (second column) channels, maximum intensity projections of selected SIM *z*-stacks are shown; the remaining images represent selected slices of SIM *z*-stacks (1,2) as shown in the schematic. Pie charts represent the distribution of replicating rDNA (grey-white, grey-cyan overlay) inside (white) or outside (cyan) the nucleolus based on signal quantification. (A) WT line containing a reduced rDNA copy number. (B) *fas1* mutant line containing a low rDNA copy number. (C) Selected details of the nucleolar rDNA replication process. Arrowheads indicate brightly DAPI-stained condensed rDNA foci inside the nucleolus.

stained by DAPI and accumulating replicating rDNA (arrows in Fig. 5C). The low rDNA copy WT line and the *fas1* mutant line showed similar replication patterns (Fig. 5A,B). During late S phase, characterised by a speckled EdU pattern, all of the active rDNA had finished replication. Interestingly, in some cells (e.g. spindle-shaped cells of the vascular system) (Fig. S4A), rDNA started to form condensed foci around the nucleolus once the replication was nearly finished, similar to the situation in the WT where the redundant rDNA copies form condensed aggregates. An analogous rDNA organisation was observed in other endopolyploid nuclei (≥4C) of plants with reduced rDNA copy number (Fig. S4B).

In conclusion, transcribed rDNA copies are not replicated at the very beginning of the S phase, but as soon as rDNA replication is initiated (during the early S phase) it lasts for the whole mid S phase until the typical speckled EdU pattern is observed.

### Inactive rDNA genes replicate from mid S until late S phase

Our analysis was performed on WT plants, although in this material active and inactive rDNA genes coexist (Chandrasekhara et al., 2016), because the low rDNA copy number lines are largely devoid of inactive copies. As shown above, *A. thaliana* S phase has three main stages, early, mid and late S phase (Fig. 2), but four different EdU labelling patterns (Figs 1 and 3) are observed when rDNA replication is evaluated. In addition, we show that more rDNA is associated with the nucleolus during the early S phase than in mid and late S phase (Fig. 4 and Table 1). In WT nuclei, once the rDNA replication is initiated in early S phase, it progresses through the

Journal of Cell Science (2018) 131, jcs202416. doi:10.1242/jcs.202416

nucleus and nucleolus simultaneously (Fig. 6A–C). In late S phase, where EdU preferentially labels heterochromatin (Fig. 6C), the replication within the nucleolus mostly ceases, with a residual replication of usually <10% (Table S4). Thus, the replication profile of rDNA can be divided into four stages: (1) very early S, with no or a very low level of rDNA replication; (2) early to mid S, with

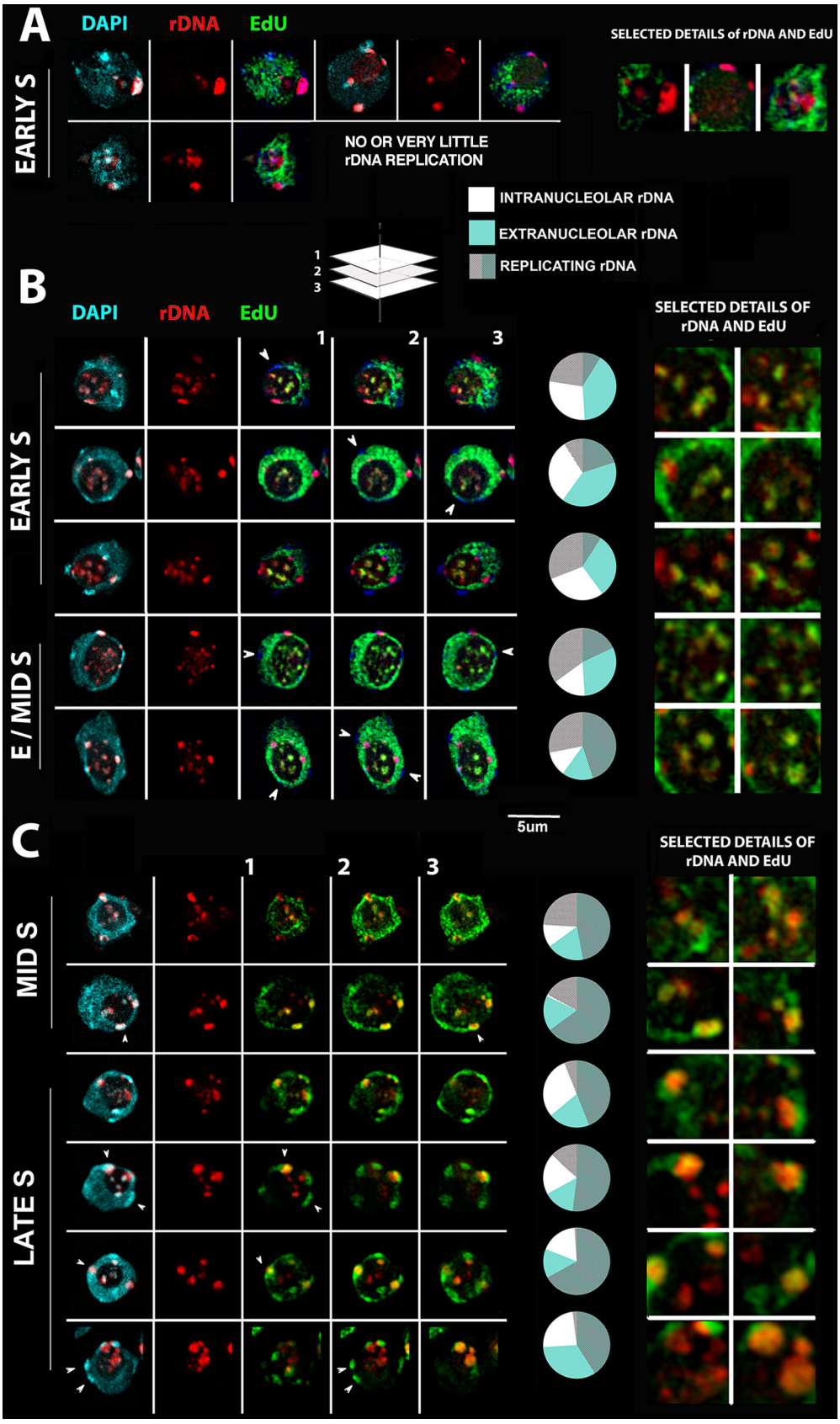


**Fig. 6. Distribution of replicating rDNA in the WT during S phase.** DAPI (cyan/blue), rDNA (AF594, red) and EdU (AF488, green) images are shown. In the DAPI and rDNA overlay (first column) and rDNA (second column) channels, maximum intensity projections of selected SIM *z*-stacks are shown; the remaining images represent selected slices of SIM *z*-stacks (1,2,3) as shown in the schematic. Arrowheads point to the chromocentres. Pie charts represent the distribution of replicating rDNA (grey-white, grey-cyan overlay) inside (white) or outside (cyan) the nucleolus based on signal quantification. Small oval extranuclear objects seen only in DAPI channel do not belong to the nuclei and likely represent bacterial contamination. (A) Very early S phase showing no or very little rDNA replication (yellow). (B) Early S and early to mid (E/Mid) S patterns. (C) Arrowheads point to the chromocentres labelled by EdU during the late S phase and forming a typical speckled pattern.

Journal of Cell Science (2018) 131, jcs202416. doi:10.1242/jcs.202416

initiation of rDNA replication, mostly inside the nucleolus; (3) mid S, with culmination of replication of active rDNA genes and initiation of replication of condensed inactive rDNA; (4) late S phase, with the finalisation of the replication in condensed rDNA foci.

## DISCUSSION

The 3D organization of the nucleus is becoming increasingly relevant to understand genome dynamics and function (Lukášová et al., 2002; Sequeira-Mendes and Gutierrez, 2015, 2016). Newly established approaches, including next-generation sequencing or chromatin conformation capture methods, have revealed the presence of several different chromatin states defined by unique combinations of chromatin marks correlating with gene activity or replication, (Feng et al., 2014; Grob et al., 2014; Kalhor et al., 2012; Roudier et al., 2011; Sequeira-Mendes et al., 2014). As already mentioned, the replication timing in mammals follows the radial model of chromatin distribution (Hatton et al., 1988; Ryba et al., 2010). There, gene-rich areas are located more centrally in the nuclei and replicate earlier than areas with a lower gene content that are found at the nuclear periphery and around the nucleolus (Cremer et al., 2001; Schardin et al., 1985). Replication time decision points are set up during the G1 phase in mammals (Dimitrova and Gilbert, 1999; Ryba et al., 2010). Although nonrandom chromatin distribution was also observed in yeast (Rodley et al., 2009), *A. thaliana* chromosome territories are more randomly distributed, with the exception of the nucleolar-organising region (NOR)-bearing chromosomes (Beven et al., 1995; Pecinka et al., 2004). Importantly, however, the replication features follow a conserved model in many aspects. Replication is initiated in regions with open chromatin containing active chromatin marks (H4 acetylation, di- or tri-methylation of H3K4, and low cytosine methylation) and the H2A.Z histone variant (Costas et al., 2011). In this study, we focused on rDNA, the most abundant repetitive genes in *A. thaliana*, and aimed to determine whether the rDNA replication timing pattern is conserved. Ribosomal DNA represents a unique mixture of active and inactive chromatin, with a considerably higher proportion of silent and condensed genes and a minor decondensed fraction found in the nucleolus (Fransz et al., 2002; Pruitt and Meyerowitz, 1986). The challenging part in determining the timing of rDNA replication lies within the rDNA organisation, which complicates the separation of active and inactive rDNA genes at the experimental level. Here, we utilised *fas1* mutant lines (Mozgova et al., 2010) and WT progeny of *fas1*×*fas2* crosses (Pavlistova et al., 2016), containing a reduced proportion of ribosomal RNA genes and largely lacking their inactive fraction, which allowed us to dissect the replication pattern of the transcriptionally active portion of rDNA from the overall rDNA replication pattern to obtain more detailed insight into rDNA replication. Our experimental strategy allowed us to obtain valuable data on the spatial and temporal organization of rDNA replication.

### rDNA replicates in the nucleolus

Transcription of ribosomal RNA genes is tightly connected with the nucleolus, as discussed elsewhere (Beven et al., 1995; Copenhaver and Pikaard, 1996; Dhar et al., 1985; Probst et al., 2004; Thiry and Thiry-Blaise, 1991). In mammals, individual, well-separated zones exist to allow for replication of rDNA in the nucleolus, where both active and inactive fractions of rDNA replicate (Dimitrova, 2011; Smirnov et al., 2014). Nucleoli of *A. thaliana* meristem cells occupy a large part of the nuclear volume (Dvořáčková et al., 2010; Pendle et al., 2005), reflecting the activity of the cell and involvement of the nucleolus in a variety of processes (reviewed in Stepiński, 2014). Extending published work that did not consider the nucleolus as a place of active replication (Hayashi et al., 2013; Yokoyama et al., 2016), we demonstrate here that the transcribed (nucleolar) fraction of rDNA remains inside the nucleolus or at the nucleolar periphery during replication. Reliable assessment of replicating DNA inside the nucleolus required EdU pulses corresponding to approximately half the time (80 min) of the estimated S phase duration (Cools et al., 2010; Hayashi et al., 2013). Nucleolar rDNA compaction is low, which per se challenges the detection limit of conventional microscopy. Thus, an improved experimental set up, including not only longer EdU pulses but also nuclei sorting and super-resolution microscopy, was necessary to uncover ongoing replication inside the nucleolus; this might possibly explain why the approaches applied previously have not been sufficient. The improved resolution of the SIM technique revealed that transcribed rDNA forms a net-like structure with the more condensed areas extensively labelled by EdU. Possibly, some islands of more compact chromatin are needed to stabilise and separate the machineries for replication and transcription in the nucleoli, or the aggregated areas of DNA/EdU signals might facilitate the formation of foci containing the factors essential for replication.

The model proposed by Gilbert and colleagues (Hiratani et al., 2009), placing expressed (early replicating) genes into the nuclear interior and inactive (late replicating) areas near the nuclear envelope, seems to partially apply to replicating *A. thaliana* rDNA. The inactive and condensed rDNA foci replicate in the nucleoplasm. However, *Arabidopsis* rDNA is recruited to the nucleolus during early S phase, while in the late phases of replication it resumes a more typical pattern with inactive loci closer to the nuclear envelope (Pontes et al., 2007; Pontvianne et al., 2012). A variety of plausible explanations for such a distribution could exist. Plant ribosomal RNA genes are, in general, highly dynamic loci (reviewed in Dvořáčková et al., 2015), frequently associating and assigned as nucleolar-associated domains (Berr and Schubert, 2007; Chandrasekhara et al., 2016; Pontvianne et al., 2016). In addition, in young seedlings the developmental silencing of inactive rDNA is not fully established (Pontes et al., 2007), and thus the increased association of rDNA with the nucleolus might relate to the general spatial reorganisation of nuclei in developing plant roots. Another possibility could be the need to activate more rDNA genes to maintain efficient rDNA transcription during the S phase while a fraction of them is being replicated. The opening of rDNA chromatin and activation of inactive genes is a frequent and well-described phenomenon in *A. thaliana*, as shown in recent studies on *fas1*, *fas2* or histone deacetylase 6 mutants as well as in WT progeny of *fas1*×*fas2* crosses (Pavlistova et al., 2016; Probst et al., 2004). However, a recent study of this topic in yeast, exploring homeostasis of gene expression during the S phase, rather speculates that mechanisms have to be employed to reduce the expression of genes once they become duplicated (Voichek et al., 2016).

It can be concluded that the *A. thaliana* nucleolus is a compartment capable of simultaneous progression of replication and transcription, similar to what is found in other systems studied (Jasencakova et al., 2001; Smirnov et al., 2014). However, whether a nucleolar localisation of rDNA is important for S phase progression remains to be elucidated, and represents a complex question not within the scope of this study. For example, the situation could be similar to that in yeast, where most of the rDNA origins fire early and origin clustering is observed, potentially explaining rDNA aggregation near the nucleolus (Pasero et al., 2002). A recent study in human cells shows that Cdc6, which is

Journal of Cell Science (2018) 131, jcs202416. doi:10.1242/jcs.202416

involved in initiation of DNA replication, is targeted to the nucleolus during late mitosis and G1 phase (Huang et al., 2016). This protein binds to the rDNA promoter and the coding regions of rRNA genes and promotes rDNA transcription initiation by facilitating RNA polymerase I transcription factor RRN3-mediated Pol I recruitment, and thus may provide a mechanism by which initiation of rDNA transcription and DNA replication can be spatially coordinated (Huang et al., 2016).

### rDNA replication takes place in four stages

Ribosomal genes in most species replicate during the whole S phase (Berger et al., 1997; Brewer and Fangman, 1988; Dimitrova, 2011; Linskens and Huberman, 1988). Early replicating regions were difficult to track before microscopy techniques for higher resolution were established (Dimitrova, 2011; Lee et al., 2010). Nevertheless, in mammals, two recent reports apparently solved this problem, showing that actively transcribed ribosomal genes (∼50% of rDNA) replicate during the first half (early and mid S), and the remaining inactive copies replicate in the second half, of the S phase (Dimitrova, 2011). Precise separation of replication and transcription is achieved by compartmentalisation of the nucleolar domains (Smirnov et al., 2014). Similarly, yeast rDNA replicates during the whole S phase (Brewer et al., 1980; Linskens and Huberman, 1988). We also show here that *A. thaliana* rDNA replicates during most of the S phase and its timing follows a model quite similar to that in other species. Three different phases (early, mid and late) can be distinguished during rDNA replication in *A. thaliana*, represented by four EdU labelling patterns: early (type 1), mid (intermediate, types 2 and 3) and late (type 4) S phase. These results are in contrast to those of other studies, which claim a biphasic S phase or consider the mid S phase as only a minor fraction (Lee et al., 2010). This discrepancy is possibly caused by inefficient separation of mid S nuclei in the previously applied experimental designs, and we overcame this problem by combining EdU labelling, FACS and *in situ* rDNA FISH.

The use of lines with a reduced number of rDNA copies, containing predominantly active rDNA, has been instrumental in revealing that active rDNA initiates replication during the early S phase and largely finishes replication before the typical late EdU pattern is established. This holds true even for the *fas1* mutants (generation 5), in which progressive loss of rDNA occurs (Mozgova et al., 2010). In WT plants, active and inactive rDNA coexist, impeding separate analysis of their replication timing. Recently, the distribution of particular rDNA variants (classified according to the variability of their external transcribed spacer region, ETS) has been described in detail (Earley et al., 2010; Havlova et al., 2016; Chandrasekhara et al., 2016; Pontvianne et al., 2007), showing that particular variants associate with active rDNA copies present on chromosome 4 (NOR4). However, NOR4 possesses much more rDNA than required for ribosome biogenesis (Mozgova et al., 2010; Pavlistova et al., 2016), and we can thus draw only limited conclusions from the observation made in the WT. It is clear that rDNA folded into chromocentres replicates during the late S phase, but an intermediate state occurs at the transition between mid S and late S. In addition, at a certain time point during mid S, replication can be detected in nearly all rDNA foci. Presumably, progression of rDNA replication occurs in a sequential manner and is accompanied by clustering of rDNA near the nucleolus.

Apparently, replication of active and inactive rDNA genes overlap during mid S phase. Whether the overlap occurs during the late S phase as well cannot be deduced from WT samples, but considering the data from lines with low rDNA copy numbers very little replication of active genes is expected during the late S phase. Altogether, we describe here in detail how rDNA replication progresses and introduce the nucleolus as an active site of rDNA replication. Whether some spatiotemporal separation of replication and transcription occurs in the *A. thaliana* nucleolus remains unanswered. Presumably concurrent transcription and replication of rDNA inside the nucleolus during the mid S phase could challenge the functionality of DNA repair pathways, but in WT plants grown under normal conditions no obvious nucleolar or nuclear DNA lesions occur as deduced from the lack of γ-H2AX foci (Amiard et al., 2011; Muchova et al., 2015). In *fas1* and *fas2* mutants, where the problem could be aggravated due to the dysfunctional nucleosome assembly (which normally stabilizes newly replicated DNA), a comparable frequency of γ-H2AX foci is found in both the nucleus and the nucleolus during replication (Muchova et al., 2015). Interestingly, in *fas1* and *fas2* mutants knockout of *RAD51B* resulted in an increase in nucleolar γ-H2AX foci, while the occurrence of nucleoplasmic foci remained at the level of *fas1* and *fas2* mutants prior to RAD51B knockout (Muchova et al., 2015). These results are consistent with the replication of active rDNA genes inside nucleoli that has been demonstrated in this study.

## MATERIALS AND METHODS

### Plant material

WT Col0 plants, *fas1* mutants (generation 5) and WT segregated from the cross between *fas1fas1* and *fas2fas2* mutants were used in this study. The *fas1* mutant plants in G5 contain 10–20% of the WT rDNA amount, and the WT (line 6) with low rDNA copy number contains ∼10%. The plant lines are described in detail in Pavlistova et al. (2016). Briefly, *fas1fas1* and *fas2fas2* plants were reciprocally crossed in generation 4 and 9, and F1 lines with the *FAS1FAS1 FAS2FAS2* genotype were selected and propagated for at least another three generations. Among these lines, two lines contained a decreased rDNA amount similar to *fas1*, which is stably maintained over generations. Of these, line 6, which displayed the lowest rDNA amount among all lines obtained, was used. WT plants expressing fibrillarin–YFP were kindly provided by Frederic Pontvianne (Laboratory of Plant Genome and Development, CNRS, Perpignan, France) (Pontvianne et al., 2013).

### Plant growth

Plants were grown on 0.5× Murashige and Skoog (MS) plates with 1% agar or in liquid media using a hydroponic system. The growth conditions were an 8-h-light–16-h-dark cycle at 22°C. For microscopy, plants were grown on agar plates only.

### EdU labelling and nuclei isolation for FACS

*A. thaliana* seedlings (4 days old) were labelled by adding 20 µM EdU (Thermo Fisher Scientific) to the liquid growth medium or by pouring the EdU solution over seedlings on plates and incubating for 40, 60 or 80 min. For microscopy, roots were fixed in 4% p-formaldehyde/1× PBS/0.5% Triton X-100 solution for 45 min, washed in PBS (2×10 min), and subjected to the Click-iT reaction in 1× PBS, 4 mM $CuSO_4$, 40 mM sodium ascorbate and 5 µM AF488 azide. For sorting, labelled root tips were excised with a scalpel and chopped with a razor blade in a modified nuclei isolation buffer (Galbraith et al., 2011) containing 45 mM $MgCl_2$, 30 mM sodium citrate, 20 mM MOPS and 0.3% Triton X-100, pH 7.0. Nuclei were subsequently filtered through 100 µm, 30 µm and eventually 10 µm filters (Partec), and fixed in solution by adding p-formaldehyde to a 2% final concentration for 12 min. Next, glycine was added to quench the p-formaldehyde (final concentration, 135 mM). Nuclei were spun down at 350 ***g*** at 4°C for 20 min, washed once in 1 ml cold 1×PBS/0.1% Triton X-100 and re-centrifuged. The pellet of nuclei was resuspended in the Click-iT reaction solution prepared according to the manufacturer's recommendations (Click-iT Plus EdU Alexa Fluor 488 Flow Cytometry Assay Kit, Thermo Fisher Scientific). The Click-iT reaction mixture was incubated for 30 min at room temperature, and then Triton X-100 was added (0.1%) and nuclei were

centrifuged (see above), washed once in cold isolation buffer and recentrifuged again. Before sorting, the pellet of nuclei was re-suspended in 400 µl cold nuclei isolation buffer and stained with DAPI (4′,6-diamidino-2-phenylindole, 2 µg/ml).

## FACS

EdU labelling was optimized by analysing the samples on a Canto II flow cytometer (BD Biosciences) (Fig. S1). Sorting of *Arabidopsis* root nuclei was performed using a FACSVantage SE (BD Biosciences) equipped with a UV laser (Coherent Enterprise II 621, Laser Innovations). Samples were sorted at a pressure of 35 psi with a 70 µm nozzle tip using a drop drive frequency of ∼40,000. The flow data rate was adjusted to keep the electronic abort <10%; typically between 500–2000 events/s. Nuclei were directly sorted onto Superfrost or Superfrost Plus slides (Menzel Glaser) in spots of 1000 nuclei each; ∼3–4 spots were sorted per slide and stored afterwards at 4°C. The fractions for sorting were classified according to their EdU content (FL1 detector Alexa 488 fluorescence BP 530/30 filter, BD Biosciences) and DNA content (DAPI fluorescence) into early, late and intermediate mid S phases. The gating strategy was as shown in Fig. 2. Briefly, in order to exclude cell debris the population of nuclei was gated out in a dot plot of side scatter (SSC) versus DAPI fluorescence (FL5 detector 505SP filter, BD Biosciences) using SSC as a threshold (Wear et al., 2016). Then, 2C, 4C, 8C and 16C populations were plotted in a DAPI-W versus DAPI-A (FL4 detector 424/44 BP filter, BD Biosciences) dot plot in order to exclude doublets. Single nuclei were finally plotted in a DAPI-A versus EdU AF488 fluorescence dot plot in which the sorting gates were defined.

## FISH

Slides containing sorted nuclei were re-fixed in 4% p-formaldehyde/1× PBS/0.5% Triton X-100 for 30 min, washed in 1× PBS (3×10 min) and treated with 100 µg/ml RNaseA (DNase-free, AppliChem) diluted in 2× SSC. Probe labelling and FISH protocols were adapted from those in Dvořáčková et al. (2010). Briefly, hybridization was performed in a 50% formamide/10% dextran sulphate/2× SSC solution. The probe and slide were denaturated for 2 min at 80°C and incubated overnight at 37°C on the sealed slides. Post-hybridisation washing steps included 3×5 min incubation with a 40% formamide/2× SSC solution at 42°C followed by 2×5 min washes in 2× SSC at 42°C. For visualization of the rDNA, the BAC clone T15P10 (AL095897/8, GenBank) was directly labelled using Alexa Fluor 594–5-dUTP (Invitrogen) or biotin 16-dUTP (Roche) and visualized by streptavidin-AF594 (Vector Laboratories).

## Microscopy

Nuclei were imaged using a Zeiss Axioimager Z1 equipped with a cooled CCD camera and appropriate filter sets (AHF Analysentechnik, http://www.ahf.de/) or a Zeiss LSM710 confocal microscope with 40×1.3 NA Oil and 63×1.4 NA Oil Plan Apochromat objectives (0.3–0.4 µm *z* steps, pinhole Airy). The root tips were imaged on a Zeiss LSM780 with a 40× C-Apochromat objective and *z*-stacks of 0.3–0.7 µm steps.

To analyse the substructures and spatial arrangement of FISH signals and chromatin beyond the classical Abbe/Raleigh limit (super-resolution), spatial 3D-structured illumination microscopy (3D-SIM) was applied using a 63×1.4 NA Oil Plan-Apochromat objective on an Elyra PS.1 microscope system (Carl Zeiss GmbH). Typically, image stacks of ∼30–50 slices with 0.1 µm spacing were acquired. The images were captured separately for each fluorochrome with the 561, 488 and 405 nm laser lines for excitation and appropriate emission filters (Weisshart et al., 2016). A resolution of up to ∼120 nm was achieved by processing the raw image stacks with Zeiss ZEN software. Image processing was performed with ImageJ (http://imagej.nih.gov/ij/).

## Image analysis

The image analysis approach was optimised according to Adler and Parmryd (2013). Acquired images were analysed in three steps: (1) segmentation of nucleolar and nuclear regions, (2) segmentation of EdU and rDNA signals, and (3) quantification of signal overlaps. Each step is detailed below. For the segmentation of nucleolar and nuclear regions, a semi-automatic approach was developed based on the DAPI channel. First, contours of the nucleolus in three different *xy* slices of each *z*-stack displaying a single cell were drawn manually, one at the centre where the nucleolus was best visible and the others at the first and last slices where the nucleolus was still visible. A full 3D binary nucleolus mask (denoted N) was computed from the three contours by interpolation. The nucleus mask was segmented by thresholding, using a triangle method (Zack et al., 1977) of the Gaussian smoothed image ($\sigma = 3$ voxels) followed by slice-by-slice morphological closing with a disk of 40 pixel diameter; the nucleolus region voxels were excluded.

For the segmentation of EdU and rDNA signals, moment-preserving thresholding (Tsai, 1985) was applied, after Gaussian smoothing with σ equaling 2 voxels. This thresholding gave the best results among all methods in ImageJ that were tested to find the maximal difference in co-occurrence of EdU and rDNA. This test was run on five images with observed colocalisation (positive control) and five images without detectable colocalisation (negative control). Similar optimization was performed to find the Gaussian smoothing parameter. The voxels after thresholding the EdU channel are denoted G and those after thresholding the rDNA channel are denoted R.

For the quantification of overlaps of different structures the sets of voxels C, N, R and G were used. For example the percentage of rDNA in the nucleolus was computed as $|R \cap N|/|R|$ or the percentage of replicating rDNA within a nucleolus as $|R \cap N \cap G|/|R \cap N|$.

The image analysis tools were programmed in MATLAB (MathWorks) using Image Processing Toolbox and DIPImage toolbox (http://www.diplib.org/).

### Acknowledgements

We thank V. Pavlištová and F. Pontvianne for providing us with necessary seeds; S. Andrade Calvo from the cytometry facility and the personnel of the microscopy facility of Centro de Biología Molecular Severo Ochoa for excellent technical support; I. Schubert for critical reading of the manuscript; and Prof. Hancock for language revision.

### Competing interests

The authors declare no competing or financial interests.

### Author contributions

Conceptualization: M.D. Methodology: M.D., B.R., J. Fuchs, V.S.; Software: P.M.; Formal analysis: P.M., M.D., V.P. Investigation: M.D.; Resources: M.D., J. Fajkus, C.G.; Data curation: P.M., M.D.; Writing - original draft: M.D.; Writing - review & editing: B.R., P.M., J. Fuchs, V.S., V.P., B.D., C.G., J. Fajkus; Visualization: V.S., M.D.; Supervision: B.D., C.G., J. Fajkus; Funding acquisition: M.D., C.G., J. Fajkus.

### Funding

This work was supported by the Czech Science Foundation (16-04166Y); the Ministry of Education, Youth and Sports of the Czech Republic, under projects of CEITEC 2020 (LQ1601) and KONTAKT II (LH15189 and LM2015062); the Ministry of Economy and Competitiveness of Spain (BFU2012-34821, BIO2013-50098 and BFU2015-68396-R to C.G.); and the Ramón Areces Foundation.

### Supplementary information

Supplementary information available online at
http://jcs.biologists.org/lookup/doi/10.1242/jcs.202416.supplemental

### References

**Adler, J. and Parmryd, I.** (2013). Colocalization analysis in fluorescence microscopy. *Methods Mol. Biol.* **931**, 97-109.

**Amiard, S., Depeiges, A., Allain, E., White, C. I. and Gallego, M. E.** (2011). Arabidopsis ATM and ATR kinases prevent propagation of genome damage caused by telomere dysfunction. *Plant Cell* **23**, 4254-4265.

**Balazs, L. and Schildkraut, C. L.** (1971). DNA replication in synchronized cultured mammalian cells. II. Replication of ribosomal cistrons in thymidine-synchronized HeLa cells. *J. Mol. Biol.* **57**, 153-158.

**Bass, H. W., Wear, E. E., Lee, T.-J., Hoffman, G. G., Gumber, H. K., Allen, G. C., Thompson, W. F. and Hanley-Bowdoin, L.** (2014). A maize root tip system to study DNA replication programmes in somatic and endocycling nuclei during plant development. *J. Exp. Bot.* **65**, 2747-2756.

**Bass, H. W., Hoffman, G. G., Lee, T.-J., Wear, E. E., Joseph, S. R., Allen, G. C., Hanley-Bowdoin, L. and Thompson, W. F.** (2015). Defining multiple, distinct, and shared spatiotemporal patterns of DNA replication and endoreduplication

from 3D image analysis of developing maize (Zea mays L.) root tip nuclei. *Plant Mol. Biol.* **89**, 339-351.
**Berger, C., Horlebein, A., Gögel, E. and Grummt, F.** (1997). Temporal order of replication of mouse ribosomal RNA genes during the cell cycle. *Chromosoma* **106**, 479-484.
**Berr, A. and Schubert, I.** (2007). Interphase chromosome arrangement in Arabidopsis thaliana is similar in differentiated and meristematic tissues and shows a transient mirror symmetry after nuclear division. *Genetics* **176**, 853-863.
**Beven, A. F., Simpson, G. G., Brown, J. W. and Shaw, P. J.** (1995). The organization of spliceosomal components in the nuclei of higher plants. *J Cell Sci* **108**, 509-518.
**Brewer, B. J. and Fangman, W. L.** (1988). A replication fork barrier at the 3′ end of yeast ribosomal RNA genes. *Cell* **55**, 637-643.
**Brewer, B. J., Zakian, V. A. and Fangman, W. L.** (1980). Replication and meiotic transmission of yeast ribosomal RNA genes. *Proc. Natl. Acad. Sci. USA* **77**, 6739-6743.
**Brown, D. D. and Gurdon, J. B.** (1964). Absence of ribosomal Rna synthesis in the anucleolate mutant of xenopus laevis. *Proc. Natl. Acad. Sci. USA* **51**, 139-146.
**Chandrasekhara, C., Mohannath, G., Blevins, T., Pontvianne, F. and Pikaard, C. S.** (2016). Chromosome-specific NOR inactivation explains selective rRNA gene silencing and dosage control in Arabidopsis. *Genes Dev.* **30**, 177-190.
**Conconi, A., Widmer, R. M., Koller, T. and Sogo, J. M.** (1989). Two different chromatin structures coexist in ribosomal RNA genes throughout the cell cycle. *Cell* **57**, 753-761.
**Cools, T., Iantcheva, A., Maes, S., Van den Daele, H. and De Veylder, L.** (2010). A replication stress-induced synchronization method for Arabidopsis thaliana root meristems. *Plant J.* **64**, 705-714.
**Copenhaver, G. P. and Pikaard, C. S.** (1996). RFLP and physical mapping with an rDNA-specific endonuclease reveals that nucleolus organizer regions of Arabidopsis thaliana adjoin the telomeres on chromosomes 2 and 4. *Plant J.* **9**, 259-272.
**Costas, C., de la Paz Sanchez, M., Stroud, H., Yu, Y., Oliveros, J. C., Feng, S., Benguria, A., López-Vidriero, I., Zhang, X., Solano, R. et al.** (2011). Genome-wide mapping of Arabidopsis thaliana origins of DNA replication and their associated epigenetic marks. *Nat. Struct. Mol. Biol.* **18**, 395-400.
**Cremer, M., von Hase, J., Volm, T., Brero, A., Kreth, G., Walter, J., Fischer, C., Solovei, I., Cremer, C. and Cremer, T.** (2001). Non-random radial higher-order chromatin arrangements in nuclei of diploid human cells. *Chromosome Res.* **9**, 541-567.
**Dhar, V. N., Miller, D. A. and Miller, O. J.** (1985). Transcription of mouse rDNA and associated formation of the nucleolus organizer region after gene transfer and amplification in Chinese hamster cells. *Mol. Cell. Biol.* **5**, 2943-2950.
**Dietzel, S., Schiebel, K., Little, G., Edelmann, P., Rappold, G. A., Eils, R., Cremer, C. and Cremer, T.** (1999). The 3D positioning of ANT2 and ANT3 genes within female X chromosome territories correlates with gene activity. *Exp. Cell Res.* **252**, 363-375.
**Dimitrova, D. S.** (2011). DNA replication initiation patterns and spatial dynamics of the human ribosomal RNA gene loci. *J. Cell Sci.* **124**, 2743-2752.
**Dimitrova, D. S. and Gilbert, D. M.** (1999). The spatial position and replication timing of chromosomal domains are both established in early G1 phase. *Mol. Cell* **4**, 983-993.
**Dvořáčková, M., Rossignol, P., Shaw, P. J., Koroleva, O. A., Doonan, J. H. and Fajkus, J.** (2010). AtTRB1, a telomeric DNA-binding protein from Arabidopsis, is concentrated in the nucleolus and shows highly dynamic association with chromatin. *Plant J.* **61**, 637-649.
**Dvořáčková, M., Fojtová, M. and Fajkus, J.** (2015). Chromatin dynamics of plant telomeres and ribosomal genes. *Plant J.* **83**, 18-37.
**Earley, K. W., Pontvianne, F., Wierzbicki, A. T., Blevins, T., Tucker, S., Costa-Nunes, P., Pontes, O. and Pikaard, C. S.** (2010). Mechanisms of HDA6-mediated rRNA gene silencing: suppression of intergenic Pol II transcription and differential effects on maintenance versus siRNA-directed cytosine methylation. *Genes Dev.* **24**, 1119-1132.
**Feng, S., Cokus, S. J., Schubert, V., Zhai, J., Pellegrini, M. and Jacobsen, S. E.** (2014). Genome-wide Hi-C analyses in wild-type and mutants reveal high-resolution chromatin interactions in Arabidopsis. *Mol. Cell* **55**, 694-707.
**Fransz, P., de Jong, J. H., Lysak, M., Castiglione, M. R. and Schubert, I.** (2002). Interphase chromosomes in Arabidopsis are organized as well defined chromocenters from which euchromatin loops emanate. *Proc. Natl. Acad. Sci. USA* **99**, 14584-14589.
**Galbraith, D. W., Janda, J. and Lambert, G. M.** (2011). Multiparametric analysis, sorting, and transcriptional profiling of plant protoplasts and nuclei according to cell type. *Methods Mol. Biol.* **699**, 407-429.
**Grob, S., Schmid, M. W. and Grossniklaus, U.** (2014). Hi-C analysis in Arabidopsis identifies the KNOT, a structure with similarities to the flamenco locus of Drosophila. *Mol. Cell* **55**, 678-693.
**Grummt, I. and Pikaard, C. S.** (2003). Epigenetic silencing of RNA polymerase I transcription. *Nat. Rev. Mol. Cell Biol.* **4**, 641-649.
**Hatton, K. S., Dhar, V., Brown, E. H., Iqbal, M. A., Stuart, S., Didamo, V. T. and Schildkraut, C. L.** (1988). Replication program of active and inactive multigene families in mammalian cells. *Mol. Cell. Biol.* **8**, 2149-2158.
**Havlová, K., Dvořáčková, M. Peiro, R., Abia, D., Mozgová, I., Vansáčová, L., Gutierrez, C. and Fajkus, J.** (2016). Variation of 45S rDNA intergenic spacers in Arabidopsis thaliana. *Plant Mol. Biol.* **92**, 457-471.
**Hayashi, K., Hasegawa, J. and Matsunaga, S.** (2013). The boundary of the meristematic and elongation zones in roots: endoreduplication precedes rapid cell expansion. *Sci. Rep.* **3**, 2723.
**Hernández, P., Lamm, S. S., Bjerknes, C. A. and Hof, J. V.** (1988). Replication termini in the rDNA of synchronized pea root cells (Pisum sativum). *EMBO J.* **7**, 303-308.
**Hiratani, I., Takebayashi, S. and Gilbert, D. M.** (2009). Replication timing and transcriptional control: beyond cause and effect–part II. *Curr. Opin. Genet. Dev.* **19**, 142-149.
**Huang, S., Xu, X., Wang, G., Lu, G., Xie, W., Tao, W., Zhang, H., Jiang, Q. and Zhang, C.** (2016). DNA replication initiator Cdc6 also regulates ribosomal DNA transcription initiation. *J. Cell Sci.* **129**, 1429-1440.
**Jacob, Y., Bergamin, E., Donoghue, M. T. A., Mongeon, V., LeBlanc, C., Voigt, P., Underwood, C. J., Brunzelle, J. S., Michaels, S. D., Reinberg, D. et al.** (2014). Selective methylation of histone H3 variant H3.1 regulates heterochromatin replication. *Science* **343**, 1249-1253.
**Jasencakova, Z., Meister, A. and Schubert, I.** (2001). Chromatin organization and its relation to replication and histone acetylation during the cell cycle in barley. *Chromosoma* **110**, 83-92.
**Kalhor, R., Tjong, H., Jayathilaka, N., Alber, F. and Chen, L.** (2012). Genome architectures revealed by tethered chromosome conformation capture and population-based modeling. *Nat. Biotechnol.* **30**, 90-98.
**Kotogány, E., Dudits, D., Horvath, G. V. and Ayaydin, F.** (2010). A rapid and robust assay for detection of S-phase cell cycle progression in plant cells and tissues by using ethynyl deoxyuridine. *Plant Methods* **6**, 5.
**Lee, T.-J., Pascuzzi, P. E., Settlage, S. B., Shultz, R. W., Tanurdzic, M., Rabinowicz, P. D., Menges, M., Zheng, P., Main, D., Murray, J. A. H. et al.** (2010). Arabidopsis thaliana chromosome 4 replicates in two phases that correlate with chromatin state. *PLoS Genet.* **6**, e1000982.
**Lima-de-Faria, A. and Jaworska, H.** (1968). Late DNA synthesis in heterochromatin. *Nature* **217**, 138-142.
**Linskens, M. H. and Huberman, J. A.** (1988). Organization of replication of ribosomal DNA in Saccharomyces cerevisiae. *Mol. Cell. Biol.* **8**, 4927-4935.
**Lukášová, E., Kozubek, S., Kozubek, M., Falk, M. and Amrichova, J.** (2002). The 3D structure of human chromosomes in cell nuclei. *Chromosome Res.* **10**, 535-548.
**Mickelson-Young, L., Wear, E., Mulvaney, P., Lee, T.-J., Szymanski, E. S., Allen, G., Hanley-Bowdoin, L. and Thompson, W.** (2016). A flow cytometric method for estimating S-phase duration in plants. *J. Exp. Bot.* **67**, 6077-6087.
**Miller, L. and Knowland, J.** (1972). Evidence for genes regulating ribosomal-Rna synthesis in xenopus-laevis embryos with partial deletions of ribosomal-rna genes. *J. Cell Biol.* **55**, A176.
**Mozgova, I., Mokros, P. and Fajkus, J.** (2010). Dysfunction of chromatin assembly factor 1 induces shortening of telomeres and loss of 45S rDNA in Arabidopsis thaliana. *Plant Cell* **22**, 2768-2780.
**Muchová, V., Amiard, S., Mozgová, I., Dvořáčková, M., Gallego, M. E., White, C. and Fajkus, J.** (2015). Homology-dependent repair is involved in 45S rDNA loss in plant CAF-1 mutants. *Plant J.* **81**, 198-209.
**Ochs, R. L., Lischwe, M. A., Spohn, W. H. and Busch, H.** (1985). Fibrillarin: a new protein of the nucleolus identified by autoimmune sera. *Biol. Cell* **54**, 123-133.
**Otero, S., Desvoyes, B., Peiró, R. and Gutierrez, C.** (2016). Histone H3 dynamics reveal domains with distinct proliferation potential in the arabidopsis root. *Plant Cell* **28**, 1361-1371.
**Pasero, P., Bensimon, A. and Schwob, E.** (2002). Single-molecule analysis reveals clustering and epigenetic regulation of replication origins at the yeast rDNA locus. *Genes Dev.* **16**, 2479-2484.
**Pavlištová, V., Dvořáčková, M., Jež, M., Mozgová, I., Mokroš, P. and Fajkus, J.** (2016). Phenotypic reversion in fas mutants of Arabidopsis thaliana by reintroduction of FAS genes: variable recovery of telomeres with major spatial rearrangements and transcriptional reprogramming of 45S rDNA genes. *Plant J.* **88**, 411-424.
**Pecinka, A., Schubert, V., Meister, A., Kreth, G., Klatte, M., Lysak, M. A., Fuchs, J. and Schubert, I.** (2004). Chromosome territory arrangement and homologous pairing in nuclei of Arabidopsis thaliana are predominantly random except for NOR-bearing chromosomes. *Chromosoma* **113**, 258-269.
**Pendle, A. F., Clark, G. P., Boon, R., Lewandowska, D., Lam, Y. W., Andersen, J., Mann, M., Lamond, A. I., Brown, J. W. and Shaw, P. J.** (2005). Proteomic analysis of the Arabidopsis nucleolus suggests novel nucleolar functions. *Mol. Biol. Cell* **16**, 260-269.
**Pontes, O., Lawrence, R. J., Silva, M., Preuss, S., Costa-Nunes, P., Earley, K., Neves, N., Viegas, W. and Pikaard, C. S.** (2007). Postembryonic establishment of megabase-scale gene silencing in nucleolar dominance. *PLoS ONE* **2**, e1157.
**Pontvianne, F., Matia, I., Douet, J., Tourmente, S., Medina, F. J., Echeverria, M. and Saez-Vasquez, J.** (2007). Characterization of AtNUC-L1 reveals a central

role of nucleolin in nucleolus organization and silencing of AtNUC-L2 gene in Arabidopsis. *Mol. Biol. Cell* **18**, 369-379.

**Pontvianne, F., Blevins, T., Chandrasekhara, C., Feng, W., Stroud, H., Jacobsen, S. E., Michaels, S. D. and Pikaard, C. S.** (2012). Histone methyltransferases regulating rRNA gene dose and dosage control in Arabidopsis. *Genes Dev.* **26**, 945-957.

**Pontvianne, F., Blevins, T., Chandrasekhara, C., Mozgová, I., Hassel, C., Pontes, O. M. F., Tucker, S., Mokros, P., Muchova, V., Fajkus, J. et al.** (2013). Subnuclear partitioning of rRNA genes between the nucleolus and nucleoplasm reflects alternative epiallelic states. *Genes Dev.* **27**, 1545-1550.

**Pontvianne, F., Carpentier, M.-C., Durut, N., Pavlištová, V., Jaske, K., Schorova, S., Parrinello, H., Rohmer, M., Pikaard, C. S., Fojtova, M. et al.** (2016). Identification of nucleolus-associated chromatin domains reveals a role for the nucleolus in 3D organization of the A. thaliana genome. *Cell Rep.* **16**, 1574-1587.

**Probst, A. V., Fagard, M., Proux, F., Mourrain, P., Boutet, S., Earley, K., Lawrence, R. J., Pikaard, C. S., Murfett, J., Furner, I. et al.** (2004). Arabidopsis histone deacetylase HDA6 is required for maintenance of transcriptional gene silencing and determines nuclear organization of rDNA repeats. *Plant Cell* **16**, 1021-1034.

**Pruitt, R. E. and Meyerowitz, E. M.** (1986). Characterization of the genome of Arabidopsis thaliana. *J. Mol. Biol.* **187**, 169-183.

**Rodley, C. D. M., Bertels, F., Jones, B. and O'Sullivan, J. M.** (2009). Global identification of yeast chromosome interactions using Genome conformation capture. *Fungal Genet. Biol.* **46**, 879-886.

**Roudier, F., Ahmed, I., Bérard, C., Sarazin, A., Mary-Huard, T., Cortijo, S., Bouyer, D., Caillieux, E., Duvernois-Berthet, E., Al-Shikhley, L. et al.** (2011). Integrative epigenomic mapping defines four main chromatin states in Arabidopsis. *EMBO J.* **30**, 1928-1938.

**Ryba, T., Hiratani, I., Lu, J., Itoh, M., Kulik, M., Zhang, J., Schulz, T. C., Robins, A. J., Dalton, S. and Gilbert, D. M.** (2010). Evolutionarily conserved replication timing profiles predict long-range chromatin interactions and distinguish closely related cell types. *Genome Res.* **20**, 761-770.

**Sequeira-Mendes, J. and Gutierrez, C.** (2015). Links between genome replication and chromatin landscapes. *Plant J.* **83**, 38-51.

**Sequeira-Mendes, J. and Gutierrez, C.** (2016). Genome architecture: from linear organisation of chromatin to the 3D assembly in the nucleus. *Chromosoma* **125**, 455-469.

**Sequeira-Mendes, J., Araguez, I., Peiro, R., Mendez-Giraldez, R., Zhang, X., Jacobsen, S. E., Bastolla, U. and Gutierrez, C.** (2014). The functional topography of the arabidopsis genome is organized in a reduced number of linear motifs of chromatin states. *Plant Cell* **26**, 2351-2366.

**Schardin, M., Cremer, T., Hager, H. D. and Lang, M.** (1985). Specific staining of human chromosomes in Chinese hamster x man hybrid cell lines demonstrates interphase chromosome territories. *Hum. Genet.* **71**, 281-287.

**Schübeler, D., Scalzo, D., Kooperberg, C., van Steensel, B., Delrow, J. and Groudine, M.** (2002). Genome-wide DNA replication profile for Drosophila melanogaster: a link between transcription and replication timing. *Nat. Genet.* **32**, 438-442.

**Schubert, V., Berr, A. and Meister, A.** (2012). Interphase chromatin organisation in Arabidopsis nuclei: constraints versus randomness. *Chromosoma* **121**, 369-387.

**Smirnov, E., Borkovec, J., Kováčik, L., Svidenská, S., Schröfel, A., Skalniková, M., Švindrych, Z., Křížek, P., Ovesný, M., Hagen, G. M. et al.** (2014). Separation of replication and transcription domains in nucleoli. *J. Struct. Biol.* **188**, 259-266.

**Stepiński, D.** (2014). Functional ultrastructure of the plant nucleolus. *Protoplasma* **251**, 1285-1306.

**Thiry, M. and Thiry-Blaise, L.** (1991). Locating transcribed and non-transcribed rDNA spacer sequences within the nucleolus by in situ hybridization and immunoelectron microscopy. *Nucleic Acids Res.* **19**, 11-15.

**Tsai, W.-H.** (1985). Moment-preserving thresholding: a new approach. *Comput. Vis. Graph. Image Process* **29**, 377-393.

**Voichek, Y., Bar-Ziv, R. and Barkai, N.** (2016). Expression homeostasis during DNA replication. *Science* **351**, 1087-1090.

**Watanabe, Y., Tenzen, T., Nagasaka, Y., Inoko, H. and Ikemura, T.** (2000). Replication timing of the human X-inactivation center (XIC) region: correlation with chromosome bands. *Gene* **252**, 163-172.

**Wear, E. E., Concia, L., Brooks, A. M., Markham, E. A., Lee, T.-J., Allen, G. C., Thompson, W. F. and Hanley-Bowdoin, L.** (2016). Isolation of plant nuclei at defined cell cycle stages using EdU labeling and flow cytometry. *Methods Mol. Biol.* **1370**, 69-86.

**Weisshart, K., Fuchs, J. and Schubert, V.** (2016). Structured illumination microscopy (SIM) and photoactivated localization microscopy (PALM) to analyze the abundance and distribution of RNA polymerase II molecules in flow sorted Arabidopsis nuclei. *Bio Protoc.* **6**:e1725.

**Yokoyama, R., Hirakawa, T., Hayashi, S., Sakamoto, T. and Matsunaga, S.** (2016). Dynamics of plant DNA replication based on PCNA visualization. *Sci. Rep.* **6**, 29657.

**Zack, G. W., Rogers, W. E. and Latt, S. A.** (1977). Automatic measurement of sister chromatid exchange frequency. *J. Histochem. Cytochem.* **25**, 741-753.